System Analysis of an Arabidopsis Mutant Altered in de Novo Fatty Acid Synthesis Reveals Diverse Changes in Seed Composition and Metabolism[1][W][OA]

Mingjie Chen, Brian P. Mooney, Martin Hajduch[2], Trupti Joshi, Mingyi Zhou, Dong Xu, and Jay J. Thelen*

Interdisciplinary Plant Group and Division of Biochemistry (M.C., B.P.M., M.H., J.J.T.), Computer Science Department (T.J., D.X.), DNA Core Microarray Facility (M.Z.), and Charles Gehrke Proteomics Center (B.P.M.), Christopher S. Bond Life Sciences Center, University of Missouri, Columbia, Missouri 65211

Embryo-specific overexpression of biotin carboxyl carrier protein 2 (BCCP2) inhibited plastid acetyl-coenzyme A carboxylase (ACCase), resulting in altered oil, protein, and carbohydrate composition in mature Arabidopsis (*Arabidopsis thaliana*) seed. To characterize gene and protein regulatory consequences of this mutation, global microarray, two-dimensional difference gel electrophoresis, iTRAQ, and quantitative immunoblotting were performed in parallel. These analyses revealed that (1) transgenic overexpression of BCCP2 did not affect the expression of three other ACCase subunits; (2) four subunits to plastid pyruvate dehydrogenase complex were 25% to 70% down-regulated at protein but not transcript levels; (3) key glycolysis and de novo fatty acid/lipid synthesis enzymes were induced; (4) multiple storage proteins, but not cognate transcripts, were up-regulated; and (5) the biotin synthesis pathway was up-regulated at both transcript and protein levels. Biotin production appears closely matched to endogenous BCCP levels, since overexpression of BCCP2 produced mostly apo-BCCP2 and the resulting ACCase-compromised, low-oil phenotype. Differential expression of glycolysis, plastid pyruvate dehydrogenase complex, fatty acid, and lipid synthesis activities indicate multiple, complex regulatory responses including feedback as well as futile "feed-forward" elicitation in the case of fatty acid and lipid biosynthetic enzymes. Induction of storage proteins reveals that oil and protein synthesis share carbon intermediate(s) and that reducing malonyl-coenzyme A flow into fatty acids diverts carbon into amino acid and protein synthesis.

During seed filling and maturation, carbon and nitrogen are stored in the form of triacylglycerols, carbohydrates, and proteins. Genetic studies in Arabidopsis (*Arabidopsis thaliana*) established that these storage reserve pathways are interconnected, although the relationship and metabolic branch point(s) are not yet clear. The *wrinkled1* (*wri1*) mutant was originally isolated based on its low seed oil content. A point mutation in WRI1, an AP2/EREB domain transcription factor, produced this phenotype and the concomitant accumulation of starch and soluble sugars (Focks and Benning, 1998; Cernac and Benning, 2004). However, seed protein content was unaffected. A mutation in the *Shrunken Seed1* (*SSE1*) gene altered seed composition by increasing starch and reducing oil and protein content (Lin et al., 2004). Mutations in metabolic pathways are also capable of dramatic changes in seed composition. An Arabidopsis mutant defective in plastidic pyruvate kinase was unable to accumulate storage oil and tocopherol (Andre and Benning, 2007). In *trehalose-6-phosphate synthase1* (*tps1*) mutant embryos, starch and sugars accumulated although protein and fatty acid levels were reduced (Gómez et al., 2006).

Transcriptome analyses of some of these mutants have begun to reveal the cascade of gene regulatory changes that result from such metabolic lesions. A transcriptome study of the *wri1* mutant, performed using a cDNA array containing more than 3,500 genes, found that approximately 1% of genes differed by more than 2-fold and most were involved in central lipid and carbohydrate metabolism (Ruuska et al., 2002). These data partly define the downstream response to disruption of the *WRI1* gene and provide a basis for comparison of the frequency of differential transcripts in response to a transcription factor that regulates glycolysis during seed development (Cernac and Benning, 2004). The transcriptome of *tps1* embryos shows coordinated down-regulation of genes involved in starch and Suc degradation and a concomitant up-regulation of genes involved in lipid mobilization and gluconeogenesis (Gómez et al., 2006). Metabolic pro-

[1] This work was supported by the National Science Foundation (Plant Genome Research Program Young Investigator award no. DBI–0332418 to J.J.T.) and by a University of Missouri Life Science Fellowship to M.C.

[2] Present address: Institute of Plant Genetics and Biotechnology, Slovak Academy of Sciences, Akademicka 2, P.O. Box 39A, SK–650 07 Nitra, Slovak Republic.

* Corresponding author; e-mail thelenj@missouri.edu.

The author responsible for distribution of materials integral to the findings presented in this article in accordance with the policy described in the Instructions for Authors (www.plantphysiol.org) is: Jay J. Thelen (thelenj@missouri.edu).

[W] The online version of this article contains Web-only data.

[OA] Open Access articles can be viewed online without a subscription.

www.plantphysiol.org/cgi/doi/10.1104/pp.108.134882

filing of *sse1* seeds found that sugars, alcohols, pyruvate, and other organic acids accumulate when carbon demand for lipid synthesis is reduced and more carbon enters the tricarboxylic acid (TCA) cycle downstream of glycolysis (Lin et al., 2006). Thus, mutations at the regulatory or substrate level can produce marked effects on seed metabolism and composition.

Seed-specific overexpression of biotin carboxyl carrier protein 2 (BCCP2) to the heteromeric plastid acetyl-coenzyme A carboxylase (ACCase) produced lower seed oil compared with nontransgenic lines (Thelen and Ohlrogge, 2002a). Immunoblot analyses with antibodies to both biotin and recombinant BCCP2 demonstrated that this phenotype was due to fractional biotinylation of BCCP2. The phenotype, therefore, was attributed to the production of nonbiotinylated ACCase complexes. Activity analysis of ACCase supported this conclusion by revealing a 3-fold reduction in ACCase activity coincident with the temporal expression of BCCP2, driven by the napin storage protein promoter (Thelen and Ohlrogge, 2002a). This mutant is unique in that it disrupts the committed step for de novo fatty acid synthesis, specifically during mid to late seed development, when enzymes of this pathway begin to accumulate (Mansfield and Briaty, 1992). The fractional nature of this ACCase mutant and its seed specificity are two beneficial characteristics of this mutant. Complete or nearly complete loss-of-function mutations for de novo fatty acid synthetic enzymes (or proteins involved in their regulation) produce lethal or retarded growth phenotypes (Shintani et al., 1997; Mou et al., 2000; Bonaventure et al., 2003; Millar et al., 2003). The lethality of knockout mutants for this pathway is likely due to the requirement of acyl chains for membrane lipid production (Thelen and Ohlrogge, 2002b). Unlike vegetative tissues, embryos principally utilize acyl chains for triacylglycerol production. Thus, collateral or pleiotropic manifestations are minimized in this ACCase mutant, allowing for direct analysis of cross talk between de novo fatty acid synthesis in the plastid and other metabolic pathways operating within developing embryos.

The varied "omic" resources available for molecular profiling differ in their target biomolecules (e.g. transcript, protein, metabolites) as well as in their sensitivity, reproducibility, and depth of coverage. Few plant systems biological investigations have studied multiple biomolecules in parallel (Gallardo et al., 2007; Sato et al., 2007). For the current study, we performed oligonucleotide microarray analyses in parallel with iTRAQ and two-dimensional difference gel electrophoresis (2D-DIGE) on this ACCase mutant. Microarrays revealed 375 differentially expressed transcripts. Parallel proteomics approaches collectively revealed a smaller number of differential proteins, some of which were not differentially regulated at the transcriptome level. Many of the protein-specific changes were confirmed by quantitative immunoblotting, suggesting that the transcriptome and proteome differences are biological rather than experimental in nature. It is evident from this study that not all proteins adhere to the assumed stoichiometric relationship between transcript and protein and that quantitative transcriptomics and proteomics, when applied together, can reveal these regulated proteins.

RESULTS

Protein, Glc, and Suc Contents Are Higher in BCCP2 Overexpression Lines

A previous study found that seed-specific overexpression of BCCP2 to the heteromeric plastid ACCase produced 24% lower seed oil compared with nontransgenic lines (Thelen and Ohlrogge, 2002a). To determine if reduced fatty acid biosynthesis in BCCP2 overexpression lines affects other seed storage reserves, protein, starch, and sugar content in mature seeds were quantified in lines 5-2 and 9-5 (Table I). Protein content in the BCCP2 overexpression lines was 10% and 25% higher in the 5-2 and 9-5 lines, respectively, while Glc and Suc levels were approximately 100% higher in both lines. Starch and Fru were not significantly affected.

2D-DIGE Analyses Reveal That Multiple Isoelectric Forms of BCCP2 Are Strongly Up-Regulated in Two Independent BCCP2 Transgenic Lines

Thirteen days after flowering (DAF), seeds were harvested from wild-type plants and two BCCP2 overexpression lines (5-2 and 9-5), and isolated protein was analyzed by 2D-DIGE (Fig. 1). The majority of proteins (approximately 1,200 spots) were equivalently expressed on both pH 3 to 10 and pH 4 to 7 gels, indicating accurate developmental staging. Twenty-three total spots were consistently differential between the wild-type and mutant lines ($P < 0.05$). Most notably, an isoelectric series of proteins at 25 kD

Table I. *Lipid, protein, and carbohydrate composition of Arabidopsis seeds from the wild type and BCCP2 overexpression lines 5-2 and 9-5*

Mean values are given in percentage of seed dry weight with SD. For lipid analysis, $n = 7$; for protein analysis, $n = 9$; and for starch, Suc, Glc, and Fru analysis, $n = 5$.

Plant	Lipid	Protein	Starch	Suc	Glc	Fru
Wild type (Columbia)	33.5 ± 0.8	31.4 ± 2.2	0.22 ± 0.08	2.2 ± 0.1	0.10 ± 0.03	0.45 ± 0.09
5-2	24.8 ± 0.6	34.7 ± 2.7	0.24 ± 0.07	3.8 ± 0.4	0.27 ± 0.05	0.41 ± 0.13
9-5	24.3 ± 0.9	39.2 ± 2.3	0.24 ± 0.08	4.9 ± 0.3	0.30 ± 0.04	0.52 ± 0.10

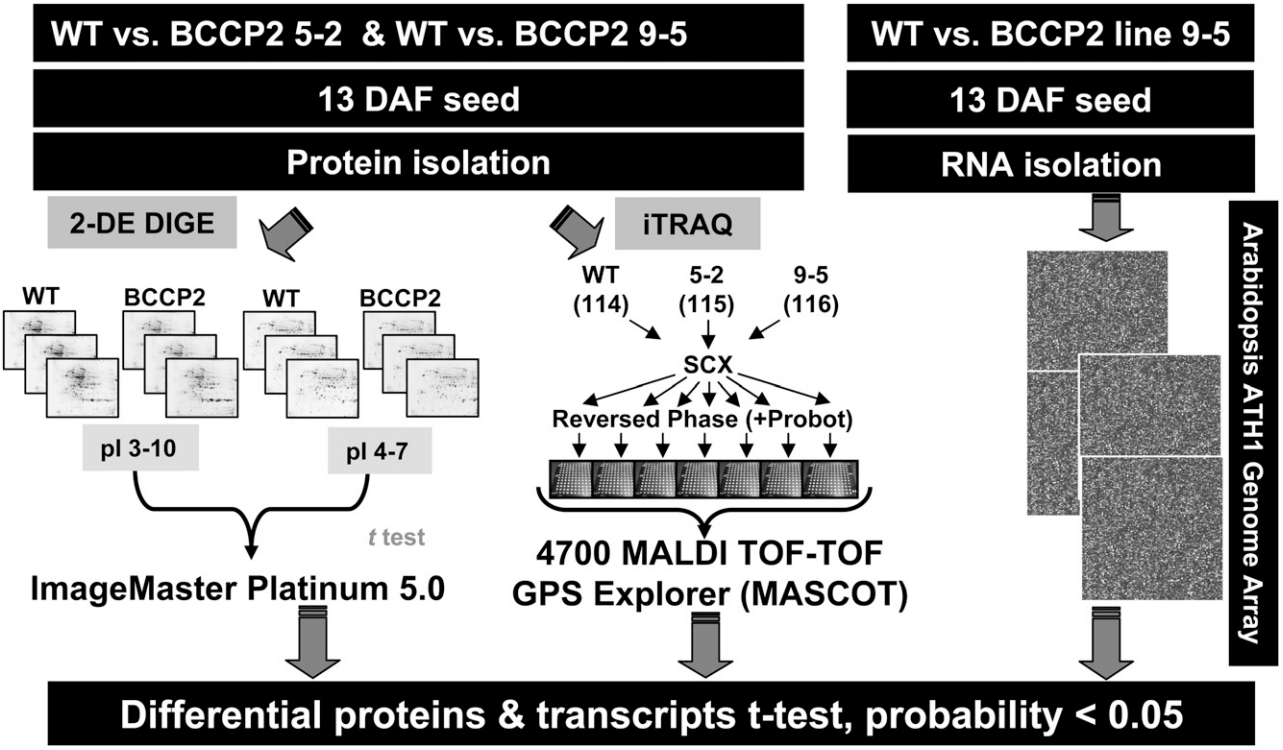

Figure 1. Experimental design used to globally analyze transcript and protein expression in BCCP2 overexpression lines. Proteins isolated from 13-DAF seeds of the wild type (WT) and BCCP2 lines 5-2 and 9-5 were analyzed in biological triplicate by 2-DE. Only those spots present on all three gels were considered for analysis. Relative quantification and expression profiles were determined using Image Master 2-DE Platinum software version 5.0. The same protein preparations also were subjected to iTRAQ analysis and quantification. For transcriptome analysis, total RNA was isolated from 13-DAF seeds of the wild type and BCCP2 line 9-5, mRNA amplified, and then hybridized with the Arabidopsis ATH1 Genome Array in duplicate. SCX, Strong cation exchange.

were up-regulated in both BCCP2 overexpression lines (Fig. 2, regions 1 and 2). A prominent but amorphous group of spots around 20 kD also appeared to be up-regulated in the BCCP2 overexpression lines (Fig. 2, B and C, circled regions). However, these spots were large and inconsistent from gel to gel and, therefore, could not be reproducibly quantified. In a global proteomic study of Arabidopsis seed filling, prominent spots in this region have been identified as napin, a 2S seed storage protein (J.J. Thelen, unpublished data).

Differentially expressed proteins were excised and digested with trypsin, and tryptic peptides were analyzed using liquid chromatography/tandem mass spectrometry (MS/MS). Seventeen of the 23 differential proteins were successfully identified in this manner (Table II). The isoelectric series of spots at 25 kD (Fig. 2, regions 1 and 2), which were up-regulated in both transgenic lines, were all identified as BCCP2. Five other spots significantly up-regulated in BCCP2 overexpression lines were identified as PSII subunits and a chlorophyll *a/b*-binding protein. A cytosolic phosphoglucomutase (At1g23190) and adenosylmethionine-8-amino-7-oxononanoate transaminase (At3g22200), which catalyzes the second step of the biotin synthesis pathway, were also up-regulated in both transgenic lines. Down-regulated proteins in both transgenic lines include plastid pyruvate dehydrogenase E3 subunit (At4g16155) and β-glucosidase (At3g21370), while ATP-dependent Clp protease (At5g50920) was reduced only in line 9-5.

Immunoblot Analyses Indicate the Presence of Five Isoelectric Species for BCCP2 and Two for BCCP1

Two functional BCCP isoforms were previously identified in Arabidopsis, BCCP1 and BCCP2 (Thelen et al., 2001). Transgenic up-regulation of BCCP2 produced multiple 25-kD isoelectric species that were identified by MS as BCCP2 (Fig. 2; Table II). This finding is surprising, since the only known posttranslational modification (PTM) for this protein is biotinylation (Thelen et al., 2001). To confirm this observation, two-dimensional electrophoresis (2-DE) protein blotting was performed with anti-BCCP2 and anti-biotin antibodies. The 2-DE immunoblot results demonstrated the presence of two distinct isoelectric species for BCCP1 (35 kD) and as many as six for BCCP2 (23–25 kD; Supplemental Fig. S1), in accordance with the

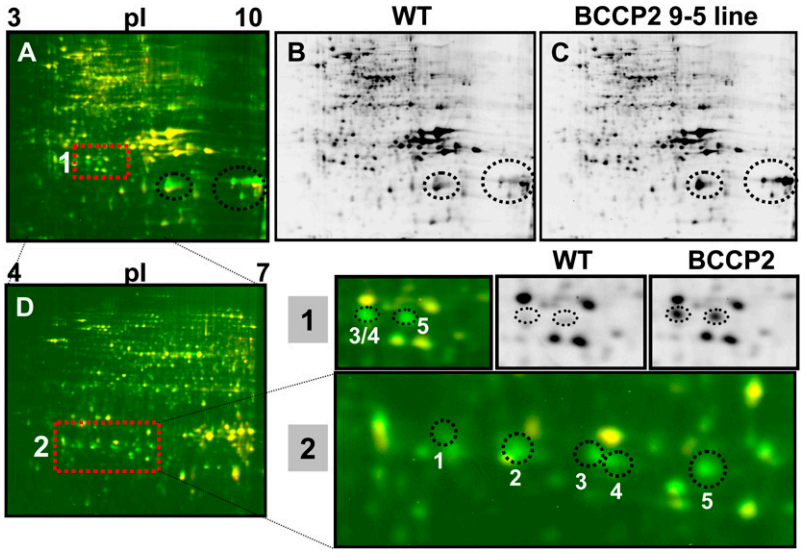

Figure 2. 2D-DIGE analysis of total protein isolated from developing seeds (13 DAF) from the wild type (WT) and BCCP2 transgenic line 9-5. Protein samples were resolved in biological triplicate from the wild type and BCCP2 overexpression lines 5-2 and 9-5 using both pH 3 to 10 (A) and pH 4 to 7 (D) immobilized pH gradient strips to maximize proteome coverage. Representative gels from a comparison of the wild type and line 9-5 are shown. A, DIGE overlay image of Cy3-red/Cy5-green channels separated on DIGE gel pH 3 to 10. B and C, Gray scale images of Cy dye-labeled protein from the wild type and BCCP2 line 9-5 from A. Highlighted regions in images B and C indicate several protein spots that were up-regulated in the BCCP2 transgenic lines but could not be resolved for quantitation. D, DIGE overlay image of Cy3-red/Cy5-green channels separated on DIGE gel pH 4 to 7. Highlighted gel regions (1 and 2) show close-ups of the boxed areas in A and D, respectively, revealing multiple up-regulated proteins at 25 kD. These protein spots were each identified as BCCP2 as indicated in Table II.

2D-DIGE results. The multiple isoelectric species for BCCP2 also showed a mass shift when analyzed by 15% SDS-PAGE: BCCP2 appeared as a doublet, while BCCP1 was a single band. The multiple isoelectric species for BCCP1 and BCCP2 could represent transcript splice variants or posttranslationally modified forms of the proteins. An extensive search of the expressed sequence tag databases revealed two splice variants for BCCP1, producing 29.6- and 26.9-kD predicted proteins with pI values of 9.57 and 10.14, respectively. No splice variants were found for BCCP2. The multiple forms of BCCP2, therefore, are likely due

Table II. *Differentially expressed proteins between wild-type and BCCP2 transgenic plants determined using 2D-DIGE*

Spot group number, protein name, Arabidopsis Genome Initiative (AGI) gene index number, and average $\log_2$ ratio of mutant (line 5-2 or 9-5) to wild-type (WT) values are indicated. Expression data are averages of biological triplicate analyses.

Spot Number	Protein Assignment	AGI Gene Index No.	Log(5-2/WT)	Log(9-5/WT)
Metabolism				
1	Biotin carboxyl carrier protein 2	At5g15530	0.56	1.73
2	Biotin carboxyl carrier protein 2	At5g15530	0.66	2.44
3	Biotin carboxyl carrier protein 2	At5g15530		5.03
4	Biotin carboxyl carrier protein 2	At5g15530	0.56	2.22
5	Biotin carboxyl carrier protein 2	At5g15530		3.66
18	Aminoacylase, putative: *N*-acyl-L-amino acid amidohydrolase	At4g38220	0.74	1.57
19	Biotin carboxyl carrier protein 2	At5g15530	0.65	0.86
23	Adenosylmethionine-8-amino-7-oxononoate transaminase	At3g22200	2.01	0.08
21	Putative β-glucosidase	At3g21370	−1.39	−1.08
30	Plastid pyruvate dehydrogenase, E3 subunit	At4g16155	−0.23	−0.12
32	Cytosolic phosphoglucomutase	At1g23190	0.30	0.47
Energy				
11	Chlorophyll *a*/*b*-binding protein/LHCII type I (LHB1B2)	At2g34420	0.52	1.40
12	PSBP-2 (PSII subunit P-2); calcium ion binding	At2g30790	0.69	0.86
13	PSBP-2 (PSII subunit P-2); calcium ion binding	At2g30790	0.76	1.00
15	PSBP-2 (PSII subunit P-2); calcium ion binding	At2g30790	0.76	0.61
28	33-kD polypeptide of oxygen-evolving complex in PSII	At5g66570	0.16	1.02
Protein modification				
20	ATP-dependent Clp protease, ATP-binding subunit	At5g50920		−0.18

to PTM, since all five were induced by a single cDNA transgene. Biotinylation, however, is not the sole PTM, since four spots were also observed with anti-biotin antibodies (Supplemental Fig. S1). Additional PTMs on BCCP2 may point toward another form of regulation for ACCase.

Gel-Free iTRAQ Analysis Identified 50 Differentially Expressed Proteins

Gel-free iTRAQ was also employed with the same protein samples used for 2D-DIGE. This approach identified one of the differential proteins also detected by 2D-DIGE (BCCP2), but mostly the data set of differentially expressed proteins was distinct from 2D-DIGE (Supplemental Table S1). iTRAQ showed a BCCP2 (At5g15530) peptide that was strongly up-regulated in line 9-5, but no iTRAQ signal was detected for line 5-2, for unclear reasons. Cruciferin and napin storage proteins were found to be 37% to 156% and 47% to 64% higher, respectively, in 5-2 and 9-5 BCCP2 lines. Putative napin 2S seed storage proteins were also higher in BCCP2 lines by 2D-DIGE (Fig. 2, B and C, circled dots), but not consistently. Plastid pyruvate dehydrogenase β-subunit (E1β; At1g30120) and plastid Fru-bisP aldolase (FBA; At3g52930) were down-regulated in BCCP2 lines, while malate dehydrogenase (At1g04410), enolase (At1g74030), and Ala-2-oxoglutarate aminotransferase 2 (AOAT2; At1g70580) were up-regulated. E1β is a subunit to the plastid pyruvate dehydrogenase complex (PDC), which produces acetyl-CoA for de novo fatty acid synthesis. Enolase catalyzes the production of phospho*enol*pyruvate, the penultimate step in glycolysis, and AOAT2 converts pyruvate into Ala. Thus, it appears that pyruvate production and steps peripheral to pyruvate production were also affected. In *Brassica napus* embryos, an alternative metabolic route for the generation of carbon for fatty acid synthesis is the Rubisco bypass (Schwender et al., 2004). Two enzymes involved in this bypass (Rubisco small subunit 1A [At1g67090] and transketolase [At3g60750]) were down-regulated in BCCP2 overexpression lines.

In contrast to the increase in storage proteins, ribosome structural constituents, Gly-rich RNA-binding proteins, and an elongation factor were down-regulated. RNA-binding proteins are involved in posttranscriptional processes such as pre-mRNA processing, splicing, RNA editing, and mRNA stability (Fedoroff, 2002). Although storage proteins increased and ribosomal proteins decreased, it should be noted that the capacity of protein synthesis (i.e. mRNA abundance) is another important factor. Since the mRNA of storage genes increases later and remains high (Ruuska et al., 2002), this could explain why storage proteins are up-regulated as the translation machinery is decreasing. Two proteins involved in chromatin modification, histone H2B (At5g22880) and ATP-dependent helicase (At1g54270), were found to be down-regulated and up-regulated, respectively, suggesting that gene regulation may take place at the chromatin level to modify transcriptional activity.

Interestingly, three oleosins were down-regulated in both BCCP2 transgenic lines. Oleosins are proteins associated with oil bodies that have been shown to play an important role in oil body structure and size, and their expression appears to be directly correlated with seed oil content (Leprince et al., 1998; Siloto et al., 2006).

Microarray Analysis Identified 375 Differential Genes

Current proteomic approaches offer only a fractional view of the proteome. In contrast, contemporary microarrays are capable of providing a nearly comprehensive assessment of the transcriptome. For comparison with the two proteomics approaches and to obtain a more inclusive assessment of collateral changes resulting from a reduction in ACCase activity in developing seeds, oligonucleotide microarrays were performed with the wild type and line 9-5. Exactly 375 of the 22,810 transcripts assayed (1.65% of the transcriptome) were differentially expressed ($P < 0.05$) between the BCCP2 9-5 line and wild-type 13-DAF seeds (Supplemental Table S2). The most prominent up-regulated transcript was BCCP2. Interestingly, none of the other nuclear-encoded ACCase subunits was differentially expressed. Transcripts for biotin synthase (Bio2; At2g43360), 7-keto-8-aminopelargonic acid (KAPA) synthase (At5g04620), and biotin/lipoic acid attachment domain-containing protein (At1g52670) were also prominently up-regulated. KAPA synthase and biotin synthase catalyze the first and last steps of the biotin synthesis pathway, respectively. Asparagine synthetase (ASN2; At5g65010), which catalyzes the formation of Asn from Asp, was also significantly up-regulated. Asn is an important nitrogen transport amino acid. Overexpression of its paralog ASN1 (At3g47340) has been reported to increase total seed protein content (Lam et al., 2003). It is possible that overexpression of ASN2 has a similar effect on storage synthesis and may contribute to the higher protein content in this mutant.

Transcripts for fatty acid synthesis and modification enzymes located downstream of ACCase (i.e. acyl carrier protein [At5g27200], acyl-ACP desaturase [At5g16240], enoyl-ACP reductase [At2g05990], β-hydroxyacyl-ACP dehydratase [At2g22230 and At5g10160], acyl-CoA desaturase [At1g06080], long-chain acyl-CoA synthetase [At1g77590], lecithin: cholesterol acyltransferase [At5g13640], and phosphatidic acid phosphatase-related [At3g15820]) were each induced in the 9-5 line. Collectively, this suggests a feed-forward or "starvation" response due to the limitation of fatty acid precursor supply for lipid synthesis. Additionally, five genes annotated as lipid transfer proteins were differentially expressed: At3g22620, At2g48140 (EDA4), and At3g22620 (LTP4) were down-regulated, while At3g51600 (LTP5) and At5g01870 (LTP6) were up-regulated.

Forty-three genes involved in carbohydrate metabolism were also differentially expressed in the BCCP2 transgenic line. Most (33 of 43 genes) showed up-regulation in the mutant. Thirteen genes for amino/organic acid metabolism were differentially expressed, and most (10 of 13) were up-regulated in the mutant. Malate dehydrogenase (At1g04410) was up-regulated at the mRNA level, in accordance with the cognate protein (Supplemental Tables S1 and S2).

A plastidic Glc-6-P/phosphate translocator (GPT; At1g61800) was transcriptionally up-regulated in the 9-5 BCCP2 overexpression line. Increased GPT expression suggests that reduced flux through fatty acid synthesis alters the subcellular partitioning of Glc-6-P between the plastid and the cytosol. How the pool size was affected in plastid and cytoplasm still remains unclear, since the direction of Glc-6-P transport must also be considered (Kammerer et al., 1998).

Interestingly, late embryogenesis-associated proteins (At3g22500, At3g22490, At2g40170, At4g36600, and At3g53040) and senescence-associated family protein (At2g17850) were down-regulated at the mRNA level (Supplemental Table S2). This finding suggests that seed maturation might be delayed in this mutant. In another low-oil mutant with a lesion in the diacylglycerol acyltransferase gene, seed maturation was delayed in comparison with the wild type (Katavic et al., 1995; Zou et al., 1999).

Quantitative Immunoblotting Confirms Omics Results

Microarray, 2D-DIGE, and gel-free iTRAQ data indicated that expression of some enzymes of glycolysis and de novo fatty acid synthesis pathways were induced when ACCase was attenuated. To confirm this observation, antibodies were developed to these proteins to quantify expression during seed development by immunoblotting. Fructokinase-1 (FK; At2g31390), plastid phosphoglycerate mutase (pdPGAM; At1g09780), cytosolic phosphoglucomutase (cytoPGM; At1g23190), and enolase (At2g36530) expression peaked at 11 DAF and then declined in wild-type seeds (Fig. 3). Expression of plastid phosphoglucomutase (pdPGM; At5g51820) and cytosolic triose-P isomerase (cytoTPI; At3g55440) peaked earlier at 9 DAF and then decreased at subsequent stages. Comparison of these trends in the wild type and two lines overexpressing BCCP2 revealed reproducible differences. Expression levels of FK and pdPGAM were approximately 50% lower in both transgenic lines at 13 and 15 DAF. In contrast, expression of cytoPGM and enolase increased between 15% and 100% in both transgenic lines at 13 and 15 DAF. No consistent changes in expression levels were observed with cytoTPI (Fig. 3). Interestingly, pdPGM was 40% to 60% down-regulated (depending upon line) at the onset of BCCP2 accumulation at 11 DAF (Fig. 3). By 13 and 15 DAF, wild-type levels of this protein were approximately 15% of the peak at 9 DAF and transgenic lines contained approximately half. Therefore, pdPGM was one of the earliest responding activities to the dominant-negative mutation in ACCase, which, given its previously established role in starch biosynthesis (Huber and Hanson, 1992; Harrison et al., 1998), suggests that it could also have regulatory/sensing roles in carbon partitioning. Glycolysis and starch synthesis diverge after the synthesis of Glc-6-P. Conversion of Glc-6-P to Glc-1-P by pdPGM commits carbon to starch synthesis. Thus, down-regulation of pdPGM will limit carbon flux into starch biosynthesis, which might explain why starch content was not higher in BCCP2 transgenic plants (Table I).

In developing seeds, there are two separate glycolysis pathways that are connected through the exchange of hexose, triose, and phospho*enol*pyruvate intermediates at the plastid envelope membrane interface (Fischer et al., 1997; Weber et al., 2000; Schneider et al., 2002). Interestingly, enzymes of these pathways show opposite expression trends in response to reduced ACCase activity: plastid enzymes decrease, while cytoplasmic enzymes increase. Remodeling of glycolysis in these two cellular compartments may help shift carbon from fatty acid synthesis to other end products. Down-regulation of plastid glycolytic enzymes was observed at 13 and 15 DAF, a 2-d delay from BCCP2 protein accumulation and ACCase activity reduction (Fig. 3). Since only a limited number of genes for cytosolic and plastid glycolysis and fatty acid synthesis were found to be differentially expressed, it is possible that these enzymes may be of regulatory importance in vivo.

The plastid PDC catalyzes the oxidative decarboxylation of pyruvate to form acetyl-CoA for de novo fatty acid synthesis in developing seeds and is composed of four subunits assembled into a complex over 4 MD in size (Mooney et al., 2002). In wild-type seeds, expression of plastid PDC subunits E1α (At1g01090), E1β (At1g30120), and E2 (At3g25820) peaked at 9 DAF, while E3 (At4g16155) peaked at 11 DAF. Compared with the wild type, all four plastid PDC subunits in both transgenic lines were coordinately reduced between 25% and 70% of wild-type levels beginning at 13 DAF, a 2-d delay from the induction of BCCP2 expression (Fig. 4).

In wild-type seeds, carboxyltransferase subunits to the heteromeric plastid ACCase showed similar expression trends as the plastid PDC subunits, while biotin carboxylase (BC; At5g35360) and BCCP2 (At5g15530) subunits were constantly expressed between 9 and 15 DAF (Fig. 5). In both BCCP2 transgenic lines, BCCP2 protein (the sum of apo- and holoproteins) was 8- to 10-fold higher than the wild type beginning at 11 DAF. Interestingly, induction and accumulation of BCCP2 had no effect on the expression of the other three subunits to ACCase (Fig. 5). At 13 and 15 DAF, expression of α-CT (At2g38040) and β-CT (Atcg00500) dropped, as did BC but to a lesser degree.

At 13 and 15 DAF, we also observed nearly 50% reduction in the expression of oleosin (Fig. 6) and greater than 2-fold up-regulation of cruciferin (CRA1;

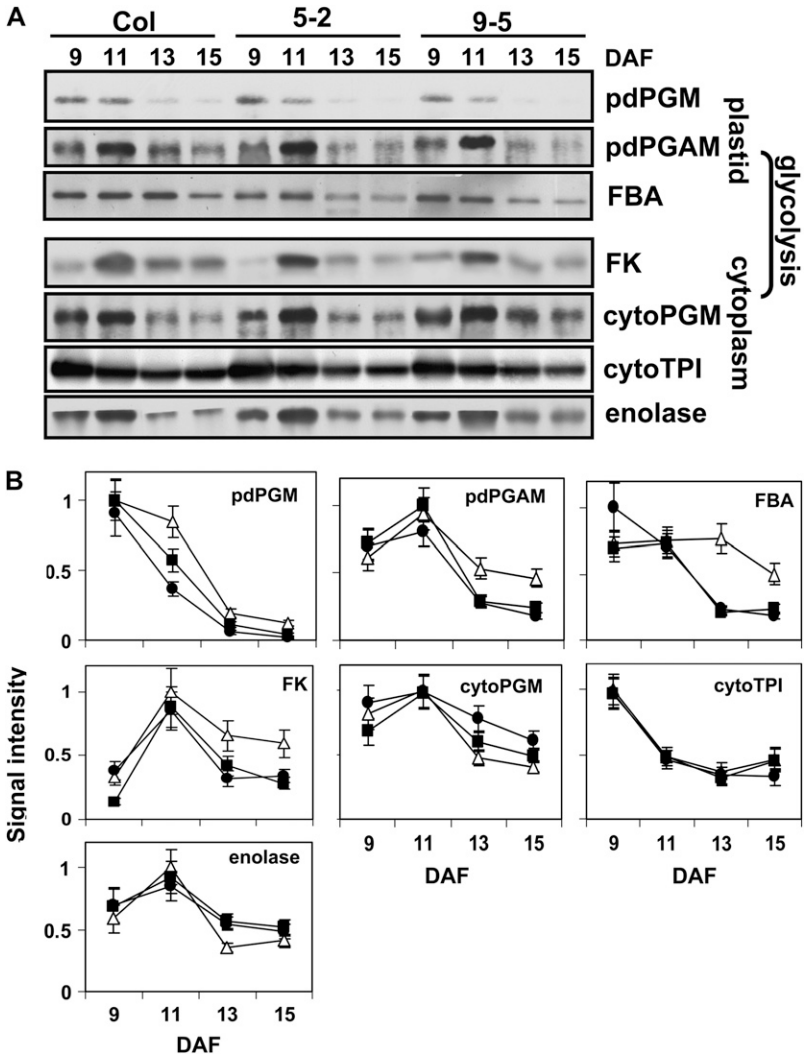

Figure 3. Quantitative immunoblot analysis of glycolytic enzymes during seed filling in Arabidopsis. A, Protein expression during seed development was detected by immunoblotting with 20 μg of protein from 9-, 11-, and 13-DAF seeds from the wild type (ecotype Columbia [Col]) and BCCP2 overexpression lines 5-2 and 9-5. B, Quantitative, densitometric analysis of protein expression from immunoblots (A) in biological triplicate. To control for blot-to-blot variation, expression data were normalized to the highest value to obtain relative units. Data points are averages of three biological replicates, and error bars indicate SD. White triangles, Wild type; black squares, 5-2; black circles, 9-5.

At5g44120) protein in both transgenic lines. These results support the 2D-DIGE and iTRAQ observations. Transcriptome data also revealed up-regulation of biotin synthesis and lipid modification enzymes at the transcriptional level (Supplemental Table S2); however, the cognate proteins were not identified as differential by either 2D-DIGE or iTRAQ, although these techniques are not comprehensive. To determine whether the cognate proteins for acyl-ACP desaturase (SAD; At5g16240), enoyl-ACP reductase (MOD1; At2g05990), β-hydroxyacyl-ACP dehydratase (BHACP; At2g22230), acyl-CoA desaturase (ADS1; At1g06080), long-chain acyl-CoA synthetase (LACS9; At1g77590), lecithin:cholesterol acyltransferase (ATPDAT; At5g13640), and phosphatidic acid phosphatase-related (PAP2; At3g15820) genes were also up-regulated, peptide antibodies were produced for quantitative immunoblotting. Additionally, a previously uncharacterized biotin attachment domain-containing protein was also up-regulated at the transcript level. We are tentatively terming this protein "BCCP-like." For the six genes with higher transcriptional level in the BCCP2 transgenic lines, four (not including BHACP or PAP2) also show higher protein levels (Fig. 7). Interestingly, SAD levels were coordinately induced with BCCP2 accumulation at 11 DAF but subsided at 13 and 15 DAF. The BCCP-like protein was also induced at 11 DAF but only in line 5-2, while in line 9-5, this protein was induced beginning at 13 DAF. BHACP showed a small but significantly higher level at 11 DAF, but this difference was not statistically significant at 13 and 15 DAF.

DISCUSSION

Targeted Genetic Perturbation to Study Metabolic Regulation in Plants

Disrupting a gene's expression and then comparing the metabolic changes between the wild type and knockout or loss-of-function mutants is a widely used approach for studying metabolic regulation. Since most metabolic activities play fundamental roles in

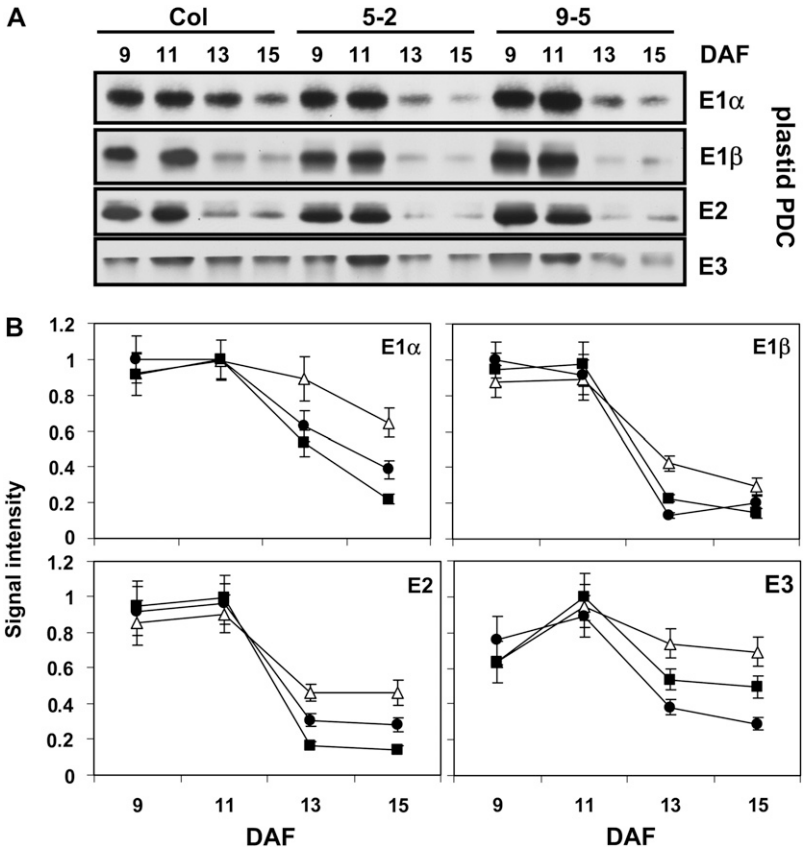

Figure 4. Quantitative immunoblot analysis of plastid PDC subunits during seed filling in Arabidopsis. A, Protein expression during seed development was detected by immunoblotting with 20 μg of protein from 9-, 11-, and 13-DAF seeds from the wild type (ecotype Columbia [Col]) and BCCP2 overexpression lines 5-2 and 9-5. E1α, E1β, E2, and E3 refer to plastid pyruvate dehydrogenase subunits. B, Quantitative, densitometric analysis of protein expression from immunoblots (A) in biological triplicate. Expression data were normalized to the highest value to obtain relative units. Data points are averages of three biological replicates, and error bars indicate SD. White triangles, Wild type; black squares, 5-2; black circles, 9-5.

cell function and therefore are expressed in multiple tissues and during different developmental stages, mutations such as T-DNA knockouts could have a profound impact on the plant, including cell death, making it difficult to distinguish between cause and consequence of the lesion (Mou et al., 2000). Conversely, other knockout mutations do not show any phenotype due to gene redundancy (Mhaske et al., 2005).

The reduced seed oil transgenic plants analyzed in this study have multiple unique properties that distinguish them from other metabolic mutants and make them attractive for studying carbon assimilation and partitioning in seeds. First, the perturbation is targeted to developing embryos instead of whole plants. Second, the disruption occurs in a rapid, temporal manner in 11-DAF seeds, approximately when reserve deposition begins. Third, protein complex activity is attenuated, not silenced, by a novel mechanism that we term "holo-protein competition." And fourth, a well-known complex, ACCase, the committed and highly regulated step for de novo fatty acid synthesis, is disrupted. However, as we are dealing with a transgenic mutation, it is possible that any phenotypic observation could be due to gene position effects. To control for this, two independent lines were analyzed. Systems biological analysis of this mutant allowed us to extract meaningful information about metabolic cross talk and the regulatory network surrounding fatty acid synthesis for oil reserve deposition in developing seeds, while eliminating the myriad pleiotropic consequences resulting from a true knockout or whole plant mutation. Even with this specific mutant, an unexpectedly complex picture emerges, which likely reflects the convoluted nature of plant metabolism.

Complementary Omics Techniques Indicate That Metabolic Regulation in Developing Seeds Occurs at Both Gene and Protein Levels

Transcriptional profiling with microarrays makes it possible to simultaneously analyze changes in mRNA levels for thousands of genes (Meyers et al., 2004). This method has already successfully confirmed that transcriptional regulation plays a major role in the control of countless processes involved in plant development and metabolism (Hennig, 2007). However, mRNA levels are not always reflective of changes in protein levels or enzyme activity; thus, this method also has its limitations (Gallardo et al., 2007; Sato et al., 2007). Proteomic approaches, on the other hand, allow one to directly investigate changes in protein expression, rather than to predict them from transcriptional data. Moreover, posttranslational modification of proteins can be directly detected using 2-DE, and when cou-

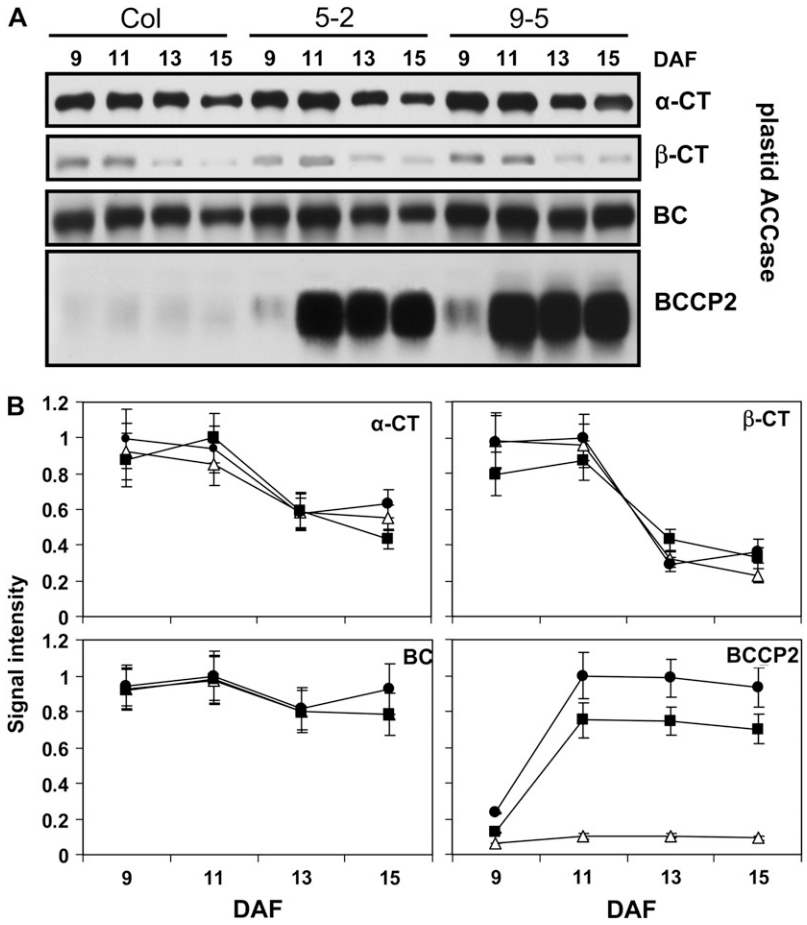

Figure 5. Quantitative immunoblot analysis of plastid ACCase subunits during seed filling in Arabidopsis. A, Protein expression during seed development was detected by immunoblotting with 20 μg of protein from 9-, 11-, and 13-DAF seeds from the wild type (ecotype Columbia [Col]) and BCCP2 overexpression lines 5-2 and 9-5. α-CT, β-CT, BC, and BCCP2 represent plastid ACCase subunits. B, Quantitative, densitometric analysis of protein expression from immunoblots (A) in biological triplicate. Expression data were normalized to the highest value to obtain relative units. Data points are averages of three biological replicates, and error bars indicate SD. White triangles, Wild type; black squares, 5-2; black circles, 9-5.

pled to DIGE, over 1,000 protein spots can be resolved with only 50 μg of protein, ideal for diminutive Arabidopsis seeds. Since enzymes are the key control mechanisms for metabolic flow, in vivo proteomic data more closely reflect the situation in planta and therefore provide better insight into metabolic processes.

However, most proteomic approaches preferentially detect abundant proteins, frequently neglecting low-copy regulatory proteins. Likewise, protein detection may be saturated for highly abundant proteins, causing the differential expression of these proteins to be underestimated. Furthermore, 2D gel electrophoresis often underrepresents proteins with extreme hydrophobicity, mass, or pI (Santoni et al., 2000; Görg et al., 2004). Therefore, non-gel-based proteomics approaches, such as iTRAQ, are also needed, as we demonstrate here. The different results obtained by 2D-DIGE, gel-free iTRAQ, and microarray analyses highlight the technical advantages and limitations of each approach while simultaneously demonstrating the need to employ multiple approaches.

Our microarray findings and those of others (Ruuska et al., 2002) show that extensive transcriptional remodeling occurs in response to the attenuation of oil synthesis in developing Arabidopsis seeds. However, only a fraction of these differentially expressed transcripts were confirmed at the protein level by 2D-DIGE and iTRAQ, perhaps reflecting the incomplete nature of these approaches. In contrast, these proteomic approaches identified some differential proteins that were unaffected transcriptionally (e.g. oleosin, cruciferin, PDC subunits). To better clarify some of these discrepancies and to verify the reliability and reproducibility of the 2D-DIGE and iTRAQ results, quantitative protein blotting was performed.

Each of the four subunits to plastid PDC was down-regulated beginning at 13 DAF without a corresponding transcriptional change; therefore, posttranslational regulation may play some role in regulating protein turnover. In humans, the E1β-subunit to mitochondrial PDC is regulated by ubiquitination and proteasome-mediated degradation (Han et al., 2008). It is possible that plants have a similar mechanism for the regulation of this complex in plastids. The apparent posttranslational decrease in oleosin expression could be due to proteolysis, although there is no prior evidence for this. Conversely, the storage protein CRA1 cruciferin might be up-regulated through a different posttranscriptional or posttranslational mechanism, perhaps related to its sequestering in a specific subcellular compartment that allows it to avoid protein turnover.

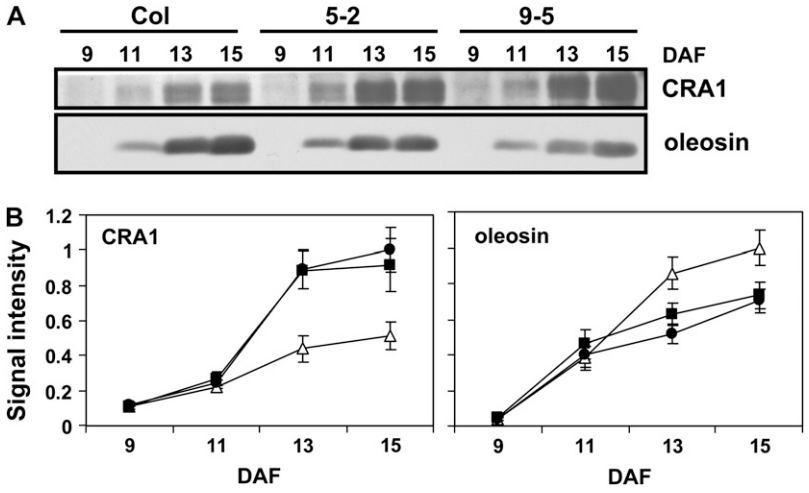

Figure 6. Quantitative immunoblot analysis of cruciferin (CRA1) and oleosin during seed filling in Arabidopsis. A, Protein expression during seed development was detected by immunoblotting with 20 μg of protein from 9-, 11-, and 13-DAF seeds from the wild type (ecotype Columbia [Col]) and BCCP2 overexpression lines 5-2 and 9-5. B, Quantitative, densitometric analysis of protein expression from immunoblots (A) in biological triplicate. Expression data were normalized to the highest value to obtain relative units. Data points are averages of three biological replicates, and error bars indicate SD. White triangles, Wild type; black squares, 5-2; black circles, 9-5.

Specific Glycolytic Activities Were Differentially Expressed in Response to Reduced Carbon Flow through de Novo Fatty Acid Synthesis

Considering the importance of glycolysis for providing acetyl-CoA precursors in developing *B. napus* embryos (Schwender and Ohlrogge, 2002), it is reasonable that glycolysis may exert distant control on fatty acid synthesis through carbon partitioning. This view is supported by a number of genetic studies. For example, mutation of pdPGM, an enzyme involved in controlling photosynthetic carbon flow in Arabidopsis, results in low oil content (Caspar et al., 1985; Periappuram et al., 2000). Similarly, a number of glycolytic enzymes (e.g. hexokinase, FK, phosphofructokinase, FBA, phosphoglycerate kinase, pdPGAM, enolase, and pyruvate kinase) were shown to be reduced in the *wri1* mutant (Focks and Benning, 1998), although activity analyses were unable to discriminate between cytosolic and plastid forms. Proteomic analysis of nearly isogenic sunflower (*Helianthus annuus*) varieties differing in seed oil content also demonstrated that glycolytic enzymes, including enolase, FK, phosphofructokinase, phosphoglycerate kinase, and cytoplasmic PGM, are up-regulated in high-oil versus low-oil varieties (Hajduch et al., 2007). In BCCP2 overexpression lines, we found plastid glycolytic enzymes (i.e. pdPGM, PGAM, and FBA) to be down-regulated at the protein level and cytosolic glycolytic enzymes (i.e., cytoPGM and enolase) to be up-regulated (Fig. 3; Table II; Supplemental Table S1). Together, these findings suggest that glycolysis and de novo fatty acid synthesis pathways cross talk in developing Arabidopsis seeds. Our results further indicate that the status of de novo fatty acid synthesis may act as a "rheostat" on the expression of glycolytic enzymes.

The Biotin Synthesis Pathway Is Up-Regulated in Response to BCCP2 Overexpression

Biotin, a water-soluble vitamin synthesized by plants, some fungi, and most bacteria, is required by all living organisms for normal cellular function and growth. Biotin is a cofactor that plays a critical role in the catalytic mechanism for a number of enzymes that are essential in both catabolic and anabolic processes (Moss and Lane, 1971). A recent study indicated that biotin has multiple roles in regulating gene expression (Che et al., 2003). Interestingly, we also observed that overexpression of BCCP2 can stimulate biotin synthesis.

The biotin synthesis pathway in plants has been established, and the precursor for this pathway is Ala (Shellhammer and Meinke, 1990; Patton et al., 1996, 1998). Differentially expressed proteins and genes mapping to the biotin synthesis pathway are shown in Supplemental Figure S2; each is elevated in response to BCCP2 overexpression. The precursor Ala has two biosynthetic routes. In developing Arabidopsis seeds, pyruvate transamination is likely the primary path, as evidenced by the up-regulation of AOAT2 (At1g70580) at the protein level in transgenic BCCP2 seeds. In contrast, no gene is affected for the second pathway, a multistep pathway that converts Cys into Ala. Overexpression of BCCP2 and the concomitant attenuation of ACCase and plastid PDC (Fig. 5) likely results in a buildup of pyruvate, which could be transaminated into Ala for biotin synthesis. This

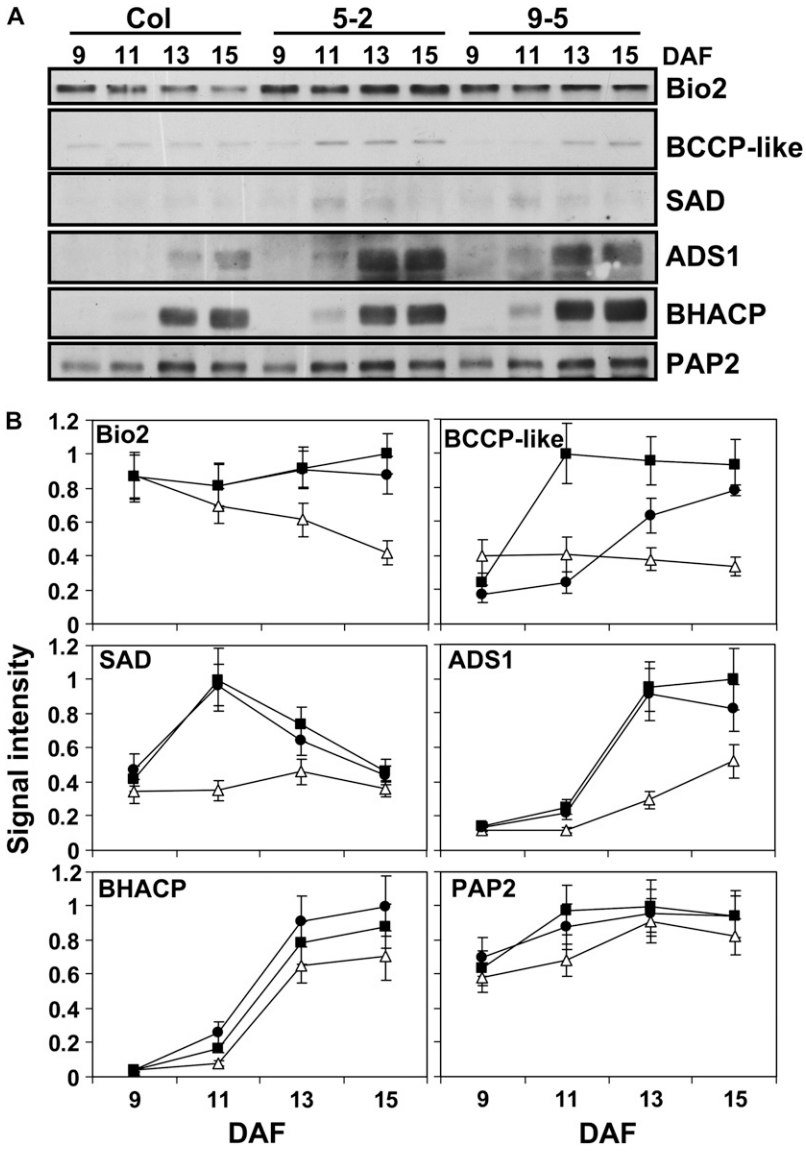

Figure 7. Quantitative analysis of enzymes involved in fatty acid synthesis and modification. A, Protein expression during seed development was detected by immunoblotting with 20 μg of protein from 9-, 11-, and 13-DAF seeds from the wild type (ecotype Columbia [Col]) and BCCP2 overexpression lines 5-2 and 9-5. B, Quantitative, densitometric analysis of protein expression from immunoblots (A) in biological triplicate. Expression data were normalized to the highest value to obtain relative units. Data points are averages of three biological replicates, and error bars indicate SD. White triangles, Wild type; black squares, 5-2; black circles, 9-5.

view is supported by the up-regulation of genes and/or proteins beginning at the aminotransferase step and continuing with almost every step in the biotin synthesis pathway (Supplemental Fig. S2). Interestingly, BCCP2 and Bio2 transcription are coordinately regulated by WRI1 during seed maturation (Baud et al., 2007). Coregulation of BCCP2 and Bio2 may allow for biotin production in vivo to closely match the principal protein and enzyme complex requiring this cofactor.

A Metabolic Shift from Oil to Storage Protein Likely Goes through the TCA Cycle

In response to reduced ACCase activity in BCCP2 overexpression lines, expression levels of all four plastid PDC subunits were reduced, presumably reducing acetyl-CoA production and thereby increasing plastid pyruvate levels. Down-regulation of the upstream plastid glycolytic proteins FBA and PGAM may further reduce carbon flow into de novo fatty acid synthesis. In contrast to plastid glycolysis, expression of cytosolic glycolytic enzymes was enhanced, which may reflect a shift in metabolism toward organic and amino acid production for increased storage protein synthesis. Due to the down-regulation of PDC and ACCase (Fig. 8), it is possible that pyruvate is converted into acetyl-CoA in the mitochondria and enters the TCA cycle by forming citrate. Up-regulation of ATP-citrate lyase (At3g06650) and cytosolic malate dehydrogenase (At1g04410) suggests that a portion of the citrate is transported into the cytoplasm to produce acetyl-CoA by ATP-citrate lyase. The oxaloacetate that is produced can also be converted into malate by cytosolic malate dehydrogenase and transported into mitochondria. The metabolic consequence is to increase TCA cycle intermediates and cytosolic acetyl-CoA. This finding is also supported by a metabolic

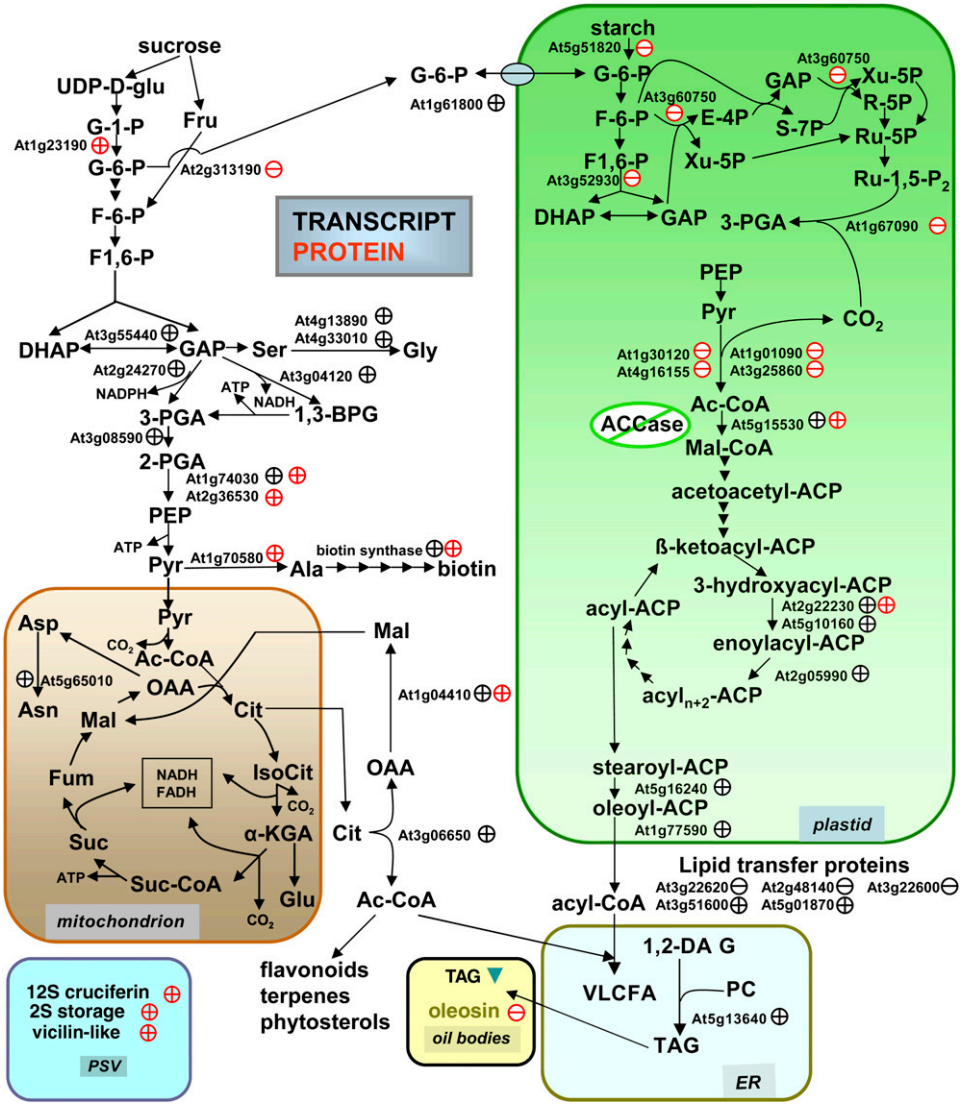

Figure 8. Summary of global transcript and protein changes resulting from overexpression of BCCP2 within developing Arabidopsis seed. The plus symbol represents up-regulation in BCCP2 overexpression lines, and the minus symbol represents down-regulation for the indicated gene or protein. Black and red symbols represent transcript and protein changes, respectively. UDP-D-glu, UDP-D-Glc; G-1-P, β-D-Glc-1-P; F-6-P, D-Fru-6-P; F1,6-P, Fru-1,6-bisP; G-6-P, β-D-Glc-6-P; DHAP, dihydroxyacetone phosphate; GAP, D-glyceraldehyde-3-P; 3-PGA, 3-phosphoglycerate; 1,3-BPG, 1,3-diphosphoglycerate; 2-PGA, 2-phosphoglycerate; PEP, phospho*enol*pyruvate; Pyr, pyruvate; Ac-CoA, acetyl-CoA; OAA, oxaloacetate; Cit, citrate; IsoCit, isocitrate; α-KGA, α-ketoglutarate; Suc-CoA, succinyl-CoA; Suc, succinate; Fum, fumarate; Mal, malate; Mal-CoA, malonyl-CoA; 1,2-DAG, 1,2-diacylglycerol; PC, phosphatidylcholine; TAG, triacylglycerol; VLCFA, very-long-chain fatty acid; E-4P, erythrose-4-P; R-5P, Rib-5-P; Ru-1,5-P_2, ribulose-1,5-bisP; Ru-5P, ribulose-5-P; S-7P, sedoheptulose-7-P; Xu-5P, xylulose-5-P; PSV, protein storage vacuole; ER, endoplasmic reticulum; FADH, flavin adenine dinucleotide.

study of *sse1*, another low-oil mutant (Lin et al., 2006). In *sse1*, a decrease in fatty acid synthesis results in an increase in carbon into the TCA cycle, causing the total amount of TCA cycle intermediates to rise (Lin et al., 2006). A partial TCA cycle model is also consistent with the carbon shift away from fumarate in the TCA cycle, as observed in the metabolic study of *sse1* (Lin et al., 2006). The TCA cycle and glycolysis help provide carbon skeletons for amino acid synthesis. The increase in TCA cycle intermediates as well as the up-regulation of aminotransferase class I and II family proteins (At5g04620; Supplemental Table S2) may increase free amino acid pools for enhanced storage protein synthesis (e.g. CRA1). Unlike the *sse1* mutant, whose total seed protein is reduced, storage protein levels in BCCP2 transgenic lines are up-regulated during development. Thus, even though both of these mutants share a similar low seed oil phenotype, the effect on storage proteins appears to be different.

Increased cytosolic acetyl-CoA production could enhance fatty acid elongation as well as the synthesis of flavonoids, terpenes, and phytosterols. Fatty acid composition analysis in BCCP2 overexpression lines revealed that $22{:}1^{\Delta 13}$ increased by 53% compared with the wild type (Thelen and Ohlrogge, 2002a), which suggests that cytosolic fatty acid elongation was enhanced. Up-regulation of flavonoid biosynthetic genes (At1g53520, At3g51240, and At1g06000), a terpene synthetic gene (At1g48800), and a sterol biosynthetic gene (At4g22756) also suggests that plastidial acetyl-CoA might be diverted from de novo fatty acid synthesis into secondary metabolic pathways (Supplemental Table S2).

Summary of Metabolic Changes Resulting from Reduced Flux through de Novo Fatty Acid Synthesis in Developing Seeds

Extensive analysis of the targeted perturbation of ACCase enzyme activity in developing seeds suggests a coordinated series of metabolic changes in response to the attenuation of fatty acid synthesis (Fig. 8). Overexpression of BCCP2 did not affect the expression of other subunits (BC, α-CT, and β-CT) in the ACCase complex. This lack of coordinated transcriptional regulation for other components in this complex is in contrast to the coordination with other enzyme complexes and in some cases pathways (e.g. biotin synthesis), and is the main reason for the dominant-negative nature of this mutation.

Fatty acid synthesis in developing seeds appears to be coordinated with precursor supply, produced by glycolysis and plastid PDC. When ACCase activity is attenuated, upstream enzymes and pathways respond, as revealed by a reduction in plastid PDC, Rubisco, and transketolase as well as an increase in cytosolic glycolytic activities. Additionally, many downstream de novo fatty acid and lipid synthesis enzymes were induced in response to the ACCase mutation.

Induction of many enzymes of the biotin synthesis pathway, in response to BCCP2 overexpression, provides another example of coordinated expression in closely related pathways (Fig. 8; Supplemental Fig. S2). This suggests that biotin synthesis and biotin-requiring proteins might undergo similar transcriptional regulation or share a transcriptional regulatory element or factor.

The major oil body protein, oleosin, was substantially down-regulated in both BCCP2 lines, although the transcript was invariant. At the same time, production of multiple storage proteins was enhanced, although no differences were observed for these genes by transcriptomics. Since storage proteins are the major protein component of mature seeds, collectively representing as much as 70% of the total protein composition in plant seeds (Hajduch et al., 2005, 2006), up-regulation of this class of proteins in addition to various amino acid biosynthetic activities (Fig. 8) appears to be the major metabolic response to reduced flux through de novo fatty acid synthesis.

MATERIALS AND METHODS

Plant Material

Wild-type and transgenic, napin-BCCP2 (T3 homozygous) Arabidopsis (*Arabidopsis thaliana* var Columbia) seeds were sown in moistened Pro-mix soil (Premier Horticulture) and grown under a 16-h-light/8-h-dark cycle, 23°C day/20°C night, 50% humidity, and light intensity of 200 μmol m^{-2} s^{-1}. Flowers were tagged prior to opening, and siliques were harvested and seeds dissected at 9, 11, 13, or 15 DAF.

Lipid, Protein, and Carbohydrate Analysis

Mature seeds were harvested and air dried for analysis. Five or eight biological replicates for each line were used, and results were expressed on a dry mass basis. Sample preparation and analysis were conducted by following the procedure described by Siloto et al. (2006).

Total RNA Isolation, RNA Amplification, Biotin Labeling, and Hybridization to the Arabidopsis ATH1 GeneChips

One microgram of seed total RNA was used to make the biotin-labeled antisense RNA (aRNA) target using the MessageAmp II-Biotin Enhanced Single Round aRNA amplification kit (Ambion) following the manufacturer's procedures. Briefly, the total RNA was reverse transcribed to first-strand cDNA with an oligo(dT) primer bearing a 5′-T7 promoter using ArrayScript reverse transcriptase. The first-strand cDNA then underwent second-strand synthesis and cleanup to become the template for in vitro transcription. Biotin-labeled aRNA was synthesized using T7 RNA transcriptase with biotin-NTP mix. After purification, aRNA was fragmented in 1× fragmentation buffer at 94°C for 35 min. Ten micrograms of fragmented aRNA in 200 μL of hybridization solution was hybridized to Arabidopsis ATH1 GeneChips (Affymetrix) at 45°C for 20 h. After hybridization, chips were washed and stained with *R*-phycoerythrin-streptavidin on Affymetrix fluidics station 450 using fluidics protocol EukGE-WS2v4. Image data were acquired by Affymetrix GeneChip scanner 3000.

Microarray Data Analysis

Microarray data analysis for the two biological replicates for each of the wild-type and napin-BCCP2 line 9-5 samples was performed using GeneSpring GX 7.3 software (Silicon Genetics). Raw data (CEL files) were loaded into GeneSpring using Robust Multichip Average preprocessing. Array intensities were normalized using data transformation to set measurements of less than 0.01 to 0.01 per chip normalization to the 50th percentile and per gene normalization to median. Normalized data were log transformed to natural log values to calculate the expression value. Scatterplots of replicate arrays made after normalization showed highly reproducible data. After normalization, criteria of Student's t test with a P value cutoff of 0.05 and 1.5-fold changes were applied to identify significantly differentially expressed genes. Exactly 375 of the 22,810 transcripts (1.65%) were differentially expressed between the BCCP2 9-5 line and the wild type.

2D-DIGE

Total protein from approximately 0.1 g of 13-DAF wild-type and napin BCCP2 (both 5-2 and 9-5 lines) seeds was isolated as described previously (Mooney and Thelen, 2004). Protein labeling with *N*-hydroxysuccinimide-activated fluorescent dyes was performed according to the manufacturer's instructions (GE Healthcare). Sample was then applied to a 24-cm immobilized pH gradient strip (GE Healthcare), focused, and resolved by 12% SDS-PAGE as described previously (Hajduch et al., 2007). Preparative 2-DE with 1 mg of protein was performed as described by Hajduch et al. (2005).

DIGE Gel Imaging, 2-DE Analysis, and Protein Identification

DIGE gels were scanned using an FLA-5000 laser scanner (Fuji Medical). Images (16 bit TIFF) were analyzed using ImageMaster 2-D Platinum software (GE Healthcare). Protein abundance was expressed as relative volume according to the normalization method provided with ImageMaster software. Statistically significant ($P < 0.05$) differentially expressed proteins were selected using the t test algorithm in ImageMaster. Differentially expressed protein spots were excised from a corresponding preparative Coomassie Brilliant Blue-stained 2-DE gel and digested by trypsin as described previously (Hajduch et al., 2005). Liquid chromatography-MS/MS using an LTQ ion trap (Thermo-Fisher) was performed as described previously for 2-DE spots (Hajduch et al., 2006).

Tandem mass spectral data were searched against the protein complement of the Arabidopsis gene index version 6. Database searches were performed on a local licensed copy of SEQUEST as part of the BioWorks 3.2SR1 software suite (Thermo-Fisher). Search parameters were as follows: enzyme, trypsin; number of internal cleavage sites, 2; mass range, 400 to 2,000; threshold, 500; minimum ion count, 35; peptide mass tolerance, 1.50; variable modification, oxidation (M); static modification, carboxyamidomethylation (C). Matching

peptides were filtered according to correlation scores (XCorr at least 1.5, 2.0, and 2.5 for +1, +2, and +3 charged peptides, respectively). For all protein assignments, a minimum of two unique, nonoverlapping peptides were required.

Peptide Labeling with iTRAQ Reagents

Protein was recovered from DIGE lysis buffer (30 mM Tris-HCl, pH 8.5, 7 M urea, 2 M thiourea, and 4% [w/v] CHAPS) by phenol extraction and methanol/ammonium acetate precipitation as described previously (Mooney and Thelen, 2004). The washed protein pellets were resuspended in buffer (8 M urea, 50 mM HEPES-KOH, pH 8.0, and 10 mM dithiothreitol) in a minimal volume and protein was quantified. An aliquot of each sample equivalent to 40 μg of protein was placed in a clean tube. Following reduction and alkylation of Cys residues and overnight trypsin digestion, iTRAQ labeling was performed according to the manufacturer's instructions (Applied Biosystems) with the following modification: in order to preserve the 60% ethanol conditions for iTRAQ labeling, each labeling reagent aliquot was resuspended in 300 μL of 100% ethanol and the entire contents of the vial was added to each sample as follows. The wild-type seed proteins were labeled with iTRAQ reagent 114, line 5-2 was labeled with reagent 115, and line 9-5 was labeled with reagent 116.

Liquid Chromatography of iTRAQ-Labeled Peptides

Following labeling, all reactions were combined and subjected to cation-exchange chromatography according to the manufacturer's instructions (iTRAQ reagent chemistry reference guide; Applied Biosystems). Six salt steps (750 μL each) were used to elute peptides from the column: 50, 100, 150, 200, 250, and 300 mM KCl in load buffer. The flow-through (unbound) fraction was also collected and analyzed. A further lyophilization step was included followed by reverse-phase column chromatography using a Dionex Ultimate 3000 HPLC system (Dionex) connected to a Probot Microfraction Collector (Dionex) for automated matrix-assisted laser-desorption ionization (MALDI) target spotting. Peptides were separated on a C18 PepMap 100 analytical column (15 cm long, 300 μm i.d., 3-μm particles; Dionex) using a continuous 30-min gradient of increasing acetonitrile. The Probot collected 400 fractions over 30 min (5 s per fraction) adding 1-cyano-4-hydroxycinnamic acid matrix (5 mg mL^{-1} final concentration) directly to the column flow. Each salt step was fractionated onto a single OptiTOF MALDI target.

MALDI-Time of Flight-Time of Flight MS Analysis of iTRAQ Peptides and Database Querying

The instrument (Applied Biosystems 4700 Proteomics Analyzer) acquired spectra from 700 to 4,000 D. Peptide calibration standards (4700 calibration mix; Applied Biosystems) were used to calibrate the instrument in MS and MS/MS modes. Sample spots were then acquired, and spectra were processed to detect peaks with signal:noise $>$ 5. Precursor ions for MS/MS were determined by a "job-wide" interpretation method as follows: signal:noise $>$ 10, all common trypsin ions excluded within a 0.5-D mass tolerance, and no retention time filtering of trypsin ions. Precursor ions were excluded if within a resolution of 200 (full width at half maximum) and a fraction-to-fraction precursor mass tolerance was set at 200 ppm. A maximum of 10 precursors were selected per spot (fraction), and the minimum chromatogram peak width was set to 2 (spots/fractions) for MS/MS acquisition with collision-induced dissociation off. The National Center for Biotechnology Information nonredundant database limited to Viridiplantae (November 24, 2007 update) was searched using the MS/MS utility of GPS Explorer version 3.6 with integrated MASCOT search engine version 2.1. All peptide data (including intensity, ion score, iTRAQ ratios, etc.) were exported to Excel for calculation of average iTRAQ ratios for proteins.

Antibody Production

To produce antibody against pdPGM (At5g51820), cytoPGM (At1g23190), TPI (At3g55440), phosphoribulokinase (At1g32060), enolase (At2g36530), FK (At2g31390), PGAM (At1g09780), and β-glucosidase (At3g21370), the gene-coding sequences were PCR amplified from their cDNA clones using the primers listed in Supplemental Table S3.

Pfu DNA polymerase (Stratagene)-generated PCR fragments were directionally cloned into the Champion pET200 TOPO vector (Invitrogen). For expression, constructs were transformed into BL21 Star (DE3) One Shot cells. Recombinant proteins were purified under native or denaturing conditions using nickel-nitrilotriacetic acid agarose (Qiagen).

For antibody production, 500 μg of recombinant protein was provided to Cocalico Biologicals for rabbit antibody production. Native cytoTPI, enolase, and FK were used as antigen, and other proteins were provided denatured. Rabbits were boosted three times before exsanguination. Antibody quality was screened by western blotting against dilutions of recombinant protein.

Peptide antibodies against BHACP (At2g22230), BCCP-like (At1g52670), PAP2 (At3g15820), Bio2 (At2g43360), ADS1 (At1g06080), SAD (At5g16240), MOD1 (At2g05990), LACS9 (At1g77590), ATPDAT (At5g13640), FBA (At3g52930), and CRA1 (At5g44120) were developed by Sigma Genosys. Peptide sequences are listed in Supplemental Table S3.

Quantitative Immunoblot Analysis of Seed Proteins

Arabidopsis seeds from different developmental stages were harvested and homogenized in 400 μL of SDS-PAGE sample buffer (60 mM Tris-HCl, pH 6.8, 60 mM SDS, 5% [v/v] glycerol, and 100 mM dithiothreitol), heated at 95°C for 5 min, and centrifuged at 15,000*g* for 10 min. Protein (20 μg) from the supernatants was resolved by SDS-PAGE and transferred to nitrocellulose under standard conditions. Blots were probed as described previously (Thelen and Ohlrogge, 2002a) using horseradish peroxidase-conjugated secondary antibody and then covered with developing buffer for 1 min (Pierce ECL western blotting substrate; Thermo Scientific), after which the solution was removed and the blots were exposed to film. Images were quantified by ImageQuant TL software (GE Healthcare). Blotting was performed in biological triplicate, and protein volumes were normalized to the highest value in the experimental series.

Supplemental Data

The following materials are available in the online version of this article.

Supplemental Figure S1. Two-dimensional gel immunoblot analyses to confirm BCCP induction and isoelectric species diversity in developing seeds of wild-type and BCCP2 overexpression lines.

Supplemental Figure S2. Biotin synthesis pathway and differentially expressed genes in the pathway.

Supplemental Table S1. Summary of differentially expressed proteins between wild-type and BCCP2 transgenic plants identified by gel-free iTRAQ.

Supplemental Table S2. Transcriptional profiling with 375 microarray-identified genes differentially expressed between the wild type and BCCP2 overexpression line 9-5 based on 1.5-fold change.

Supplemental Table S3. Oligonucleotide primers and synthetic peptides used for heterologous expression of Arabidopsis proteins and peptide antibody production, respectively.

ACKNOWLEDGMENT

We thank Melody Kroll for editing this manuscript.

Received December 30, 2008; accepted February 27, 2009; published March 11, 2009.

LITERATURE CITED

Andre C, Benning C (2007) Arabidopsis seedlings deficient in a plastidic pyruvate kinase are unable to utilize seed storage compounds for germination and establishment. Plant Physiol **145:** 1670–1680

Baud S, Mendoza MS, To A, Harscoët E, Lepiniec L, Dubreucq B (2007) WRINKLED1 specifies the regulatory action of LEAFY COTYLEDON2 towards fatty acid metabolism during seed maturation in Arabidopsis. Plant J **50:** 825–838

Bonaventure G, Salas JJ, Pollard MR, Ohlrogge JB (2003) Disruption of the *FATB* gene in *Arabidopsis* demonstrates an essential role of saturated fatty acids in plant growth. Plant Cell **15:** 1020–1033

Caspar T, Huber SC, Somerville C (1985) Alteration in growth, photosynthesis, and respiration in a starchless mutant of *Arabidopsis thaliana* (L.) deficient in chloroplast phosphoglucomutase activity. Plant Physiol **79:** 11–17

Cernac A, Benning C (2004) *Wrinkled1*encodes an AP2/EREB domain protein involved in the control of storage compound biosynthesis in *Arabidopsis*. Plant J **40:** 575–585

Che P, Weaver LM, Wurtele ES, Nikolau BJ (2003) The role of biotin in regulating 3-methylcrotonyl coenzyme A carboxylase expression in Arabidopsis. Plant Physiol **131:** 1479–1486

Fedoroff NV (2002) RNA-binding proteins in plants: the tip of an iceberg? Curr Opin Plant Biol **5:** 452–459

Fischer K, Kammerer B, Gutensohn M, Arbinger B, Weber A, Häusler RE, Flügge UI (1997) A new class of plastidic phosphate translocators: a putative link between primary and secondary metabolism by the phosphoenolpyruvate/phosphate antiporter. Plant Cell **9:** 453–462

Focks N, Benning C (1998) *Wrinkled1*: a novel, low-seed-oil mutant of Arabidopsis with a deficiency in the seed-specific regulation of carbohydrate metabolism. Plant Physiol **118:** 91–101

Gallardo K, Firnhaber C, Zuber H, Héricher D, Belghazi M, Henry C, Küster H, Thompson R (2007) A combined proteome and transcriptome analysis of developing *Medicago truncatula* seeds. Mol Cell Proteomics **6:** 2165–2179

Gómez LD, Baud S, Gilday A, Graham IA (2006) Delayed embryo development in the *ARABIDOPSIS TREHALOSE-6-PHOSPHATE SYNTHASE 1* mutant is associated with altered cell wall structure, decreased cell division and starch accumulation. Plant J **46:** 69–84

Görg A, Weiss W, Dunn MJ (2004) Current two-dimensional electrophoresis technology for proteomics. Proteomics **4:** 3665–3685

Hajduch M, Casteel JE, Hurrelmeyer KE, Zhang S, Agrawal GK, Thelen JJ (2006) Proteomic analysis of seed filling in *Brassica napus*: developmental characterization of metabolic isozymes using high-resolution two-dimensional gel electrophoresis. Plant Physiol **141:** 32–46

Hajduch M, Casteel JE, Tang SX, Hearne LB, Knapp S, Thelen JJ (2007) Proteomic analysis of near-isogenic sunflower varieties differing in seed oil traits. J Proteome Res **6:** 3232–3241

Hajduch M, Ganapathy A, Stein JW, Thelen JJ (2005) A systematic proteomic study of seed filling in soybean: establishment of high-resolution two-dimensional reference maps, expression profiles, and an interactive proteome database. Plant Physiol **137:** 1397–1419

Han Z, Zhong L, Srivastava A, Stacpoole PW (2008) Pyruvate dehydrogenase complex deficiency caused by ubiquitination and proteasome-mediated degradation of the E1β subunit. J Biol Chem **283:** 237–243

Harrison C, Hedley C, Wang T (1998) Evidence that the rug3 locus of pea (Pisum sativum L.) encodes plastidial phosphoglucomutase confirms that the imported substrate for starch synthesis in pea amyloplasts is glucose-6-phosphate. Plant J **13:** 753–762

Hennig L (2007) Patterns of beauty: omics meets plant development. Trends Plant Sci **12:** 287–293

Huber S, Hanson K (1992) Carbon partitioning and growth of a starchless mutation of *Nicotiana sylvestris*. Plant Physiol **99:** 1449–1454

Kammerer B, Fisher K, Hilpert B, Schuber S, Gutensohn M, Weber A, Flügge UI (1998) Molecular characterization of a carbon transport in plastids from heterotrophic tissues: the glucose 6-phosphate/phosphate antiporter. Plant Cell **10:** 105–117

Katavic V, Reed DW, Taylor DC, Giblin EM, Barton DL, Zou J, MacKenzie SL, Covello PS, Kunst L (1995) Alteration of seed fatty acid composition by an ethyl methanesulfonate-induced mutation in *Arabidopsis thaliana* affecting diacylglycerol acyltransferase activity. Plant Physiol **108:** 399–409

Lam HM, Wong P, Chan HK, Yam KM, Chen L, Chow CM, Coruzzi GM (2003) Overexpression of the *ASN1*gene enhances nitrogen status in seeds of Arabidopsis. Plant Physiol **132:** 926–935

Leprince O, van Aelst AC, Pritchard HW, Murphy DJ (1998) Oleosins prevent oil-body coalescence during seed imbibition as suggested by a low-temperature scanning electron microscope study of desiccation-tolerant and -sensitive oilseeds. Planta **204:** 109–119

Lin Y, Cluette-Brown JE, Goodman HM (2004) The peroxisome deficient Arabidopsis mutant sse1 exhibits impaired fatty acid synthesis. Plant Physiol **135:** 814–827

Lin Y, Ulanov AV, Lozovaya V, Widholm J, Zhang G, Guo J, Goodman HM (2006) Genetic and transgenic perturbations of carbon reserve production in Arabidopsis seeds reveal metabolic interactions of biochemical pathways. Planta **225:** 153–164

Mansfield SG, Briaty LG (1992) Cotyledon cell development in Arabidopsis thaliana during reserve deposition. Can J Bot **70:** 151–164

Meyers B, Galbraith D, Nelson T, Agrawal V (2004) Methods for transcriptional profiling in plants: be fruitful and replicate. Plant Physiol **135:** 637–652

Mhaske V, Beldjilali K, Ohlrogge J, Pollard M (2005) Isolation and characterization of an Arabidopsis thaliana knockout line for phospholipid:diacylglycerol transacylase gene (At5g13640). Plant Physiol Biochem **43:** 413–417

Millar A, Wrischer M, Kunst L (2003) Accumulation of very-long-chain fatty acids in membrane glycerolipids is associated with dramatic alterations in plant morphology. Plant Cell **10:** 1889–1902

Mooney BP, Miernyk JA, Randall DD (2002) The complex fate of alpha-ketoacids. Annu Rev Plant Biol **53:** 357–375

Mooney BP, Thelen JJ (2004) High-throughput peptide mass fingerprinting of soybean seed proteins: automated workflow and utility of UniGene expressed sequence tag databases for protein identification. Phytochemistry **65:** 1733–1744

Moss J, Lane MD (1971) The biotin-dependent enzymes. Adv Enzymol **35:** 321–442

Mou Z, He Y, Dai Y, Liu X, Li J (2000) Deficiency in fatty acid synthase leads to premature cell death and dramatic alterations in plant morphology. Plant Cell **12:** 405–417

Patton DA, Schetter AL, Franzmann LH, Nelson K, Ward ER, Meinke DW (1998) An embryo-defective mutant of Arabidopsis disrupted in the final step of biotin synthesis. Plant Physiol **116:** 935–946

Patton DA, Volrath S, Ward ER (1996) Complementation of the bio 1 Arabidopsis biotin auxotroph with a bacterial biotin biosynthetic gene. Mol Gen Genet **251:** 261–266

Periappuram C, Steinhauer L, Barton DL, Taylor DC, Chatson B, Zou JT (2000) The plastidic phosphoglucomutase from Arabidopsis: a reversible enzyme reaction with an important role in metabolic control. Plant Physiol **122:** 1193–1199

Ruuska SA, Girke T, Benning C, Ohlrogge JB (2002) Contrapuntal network of gene expression during *Arabidopsis* seed filling. Plant Cell **14:** 1191–1206

Santoni V, Molloy M, Rabilloud T (2000) Un amour impossible? Electrophoresis **21:** 1054–1070

Sato A, Miyazaki E, Satake A, Hiramoto A, Hiraoka O, Miyake T, Kim H, Wataya Y (2007) Proteome and transcriptome analysis of cell death induced by 5-fluoro-2′-deoxyuridine. Nucleic Acids Symp Ser **51:** 433–434

Schneider A, Häusler RE, Kolukisaoglu U, Kunze R, van der Graaff E, Schwacke R, Catoni E, Desimone M, Flügge UI (2002) An Arabidopsis thaliana knock-out mutant of the chloroplast triose phosphate/phosphate translocator is severely compromised only when starch synthesis, but not starch mobilisation is abolished. Plant J **32:** 685–699

Schwender J, Goffman F, Ohlrogge JB, Shachar-Hill Y (2004) Rubisco without the Calvin cycle improves the carbon efficiency of developing green seeds. Nature **432:** 779–782

Schwender J, Ohlrogge JB (2002) Probing in vivo metabolism by stable isotope labeling of storage lipid and proteins in developing *Brassica napus* embryos. Plant Physiol **130:** 347–361

Shellhammer J, Meinke D (1990) Arrested embryos from the bio 1 auxotroph of *Arabidopsis thaliana* contain reduced levels of biotin. Plant Physiol **93:** 1162–1167

Shintani D, Roesler K, Shorrosh B, Savage L, Ohlrogge JB (1997) Antisense expression and overexpression of biotin carboxylase in tobacco leaves. Plant Physiol **114:** 881–886

Siloto RMP, Findlay K, Lopez-Villalobos A, Yeung EC, Nykiforuk CL, Moloney MM (2006) The accumulation of oleosins determines the size of seed oilbodies in *Arabidopsis*. Plant Cell **18:** 1961–1974

Thelen JJ, Mekhedov S, Ohlrogge JB (2001) Brassicaceae express multiple isoforms of biotin carboxyl carrier protein in a tissue-specific manner. Plant Physiol **125:** 2016–2028

Thelen JJ, Ohlrogge JB (2002a) Both antisense and sense expression of biotin carboxyl carrier protein isoform 2 inactivates the plastid acetyl-coenzyme A carboxylase in *Arabidopsis thaliana*. Plant J **32:** 419–431

Thelen JJ, Ohlrogge JB (2002b) Metabolic engineering of fatty acid biosynthesis in plants. Metabolic Engineering J **4:** 12–21

Weber A, Servaites JC, Geiger DR, Kofler H, Hille D, Gröner F, Hebbeker U, Flügge UI (2000) Identification, purification, and molecular cloning of a putative plastidic glucose translocator. Plant Cell **12:** 787–802

Zou J, Wei Y, Jako C, Kumar A, Selvaraj G, Taylor DC (1999) The *Arabidopsis thaliana* TAG1 mutant has a mutation in a diacylglycerol acyltransferase gene. Plant J **19:** 645–653